Chemie Ingenieur Technik

Chemie Ingenieur Technik

RESEARCH ARTICLE OPEN ACCESS

Synthesis of Hydrocarbon Fuels From Dimethyl Ether Through Co-Oligomerization of Olefins

Marc Pfennings | Gia Trung Hoang | Ravi Teja Ganti | Julian Dutzi | Ulrich Arnold | Jörg Sauer

Karlsruhe Institute of Technology, Institute of Catalysis Research and Technology, Eggenstein-Leopoldshafen, Germany

Correspondence: Ulrich Arnold (ulrich.arnold@kit.edu)

Received: 16 December 2025 | **Revised:** 27 March 2026 | **Accepted:** 30 March 2026

Keywords: dimethyl ether | heterogeneous catalysis | olefins | oligomerization | sustainable aviation fuels

ABSTRACT

This work investigates the impact of higher olefins and typical impurities from a preceding Dimethyl ether-to-Olefins (DtO) process on olefin oligomerization for fuel production. Feed complexity was systematically increased to mimic a DtO product containing lower and higher olefins as well as paraffinic and aromatic components. Higher olefins incorporation enhanced the yield of C_{13+} hydrocarbons, while impurities reduced it. Kerosene was the dominant product fraction. Temperature was determined to be the governing parameter for promoting C_{13+} formation and increasing diesel fuel yields, surpassing feed composition effects. Several key properties of the kerosene fraction comply with the ASTM D7566 22a standard for sustainable aviation fuels, whereas some important properties of the diesel fraction meet the ISO 8217 DMB grade for marine diesel fuel.

1 | Introduction

Through the "Hightech Agenda Germany," the German government aims to promote sustainable fuel production in order to reduce CO_2 emissions [1]. One promising approach towards achieving these objectives is the oligomerization of olefins to produce hydrocarbons within the gasoline, jet, or diesel fuel boiling ranges. Olefins can be produced by converting methanol via the Methanol-to-Olefins (MtO) process or dimethyl ether (DME) via the DME-to-Olefins (DtO) process [2, 3]. DME shows advantageous thermodynamic and economical properties compared to methanol [2, 4], as DME can be synthesized directly from syngas with a lower H_2/CO ratio [5, 6] or a high CO_2 content [7, 8]. Additionally, DME is generally more reactive than methanol [9, 10]. Furthermore, the DtO process produces less water [11] and is less exothermic than the MtO process [2, 12].

Regarding the catalysts for MtO/DtO processes, zeolites with the MFI framework type or silicoaluminophosphates (SAPO) have been mostly utilized, resulting predominantly in C_2–C_4 olefins [2, 3, 13, 14]. Recently, a *MRE zeolite caused a significant change in the product distribution by also forming higher olefins up to C_{11} [15]. When the *MRE catalyst was loaded with palladium and hydrogen was co-fed during DME conversion, the catalyst lifetime increased markedly, resulting in a cumulative conversion capacity exceeding 800 $g_{DME}\ g^{-1}{}_{cat}$ [16, 17]. At the same time, the ethylene and aromatics contents remained low. This is particularly advantageous for subsequent oligomerization towards jet and diesel-range fuels since ethylene predominantly forms lighter oligomers and promotes side reactions associated with aromatics and coke formation [18–21].

The homo-oligomerization of individual lower olefin species like propylene and butylenes for the production of fuels, especially gasoline, is well studied and industrially established [18–24]. Processes such as UOP's Catpoly and ExxonMobil's Mobil Olefins to Gasoline and Distillate (MOGD) utilize mainly C_3–C_4 olefin feeds to produce high-octane gasoline and some distillate-range

Abbreviations: AtJ, alcohol-to-jet; DMB, distillate marine fuel grade B; DME, dimethyl ether; DtO, DME-to-olefins; FID, flame ionization detector; GC, gas chromatography; MtO, methanol-to-olefins; SAF, sustainable aviation fuels; SAPO, silicoaluminophosphates.

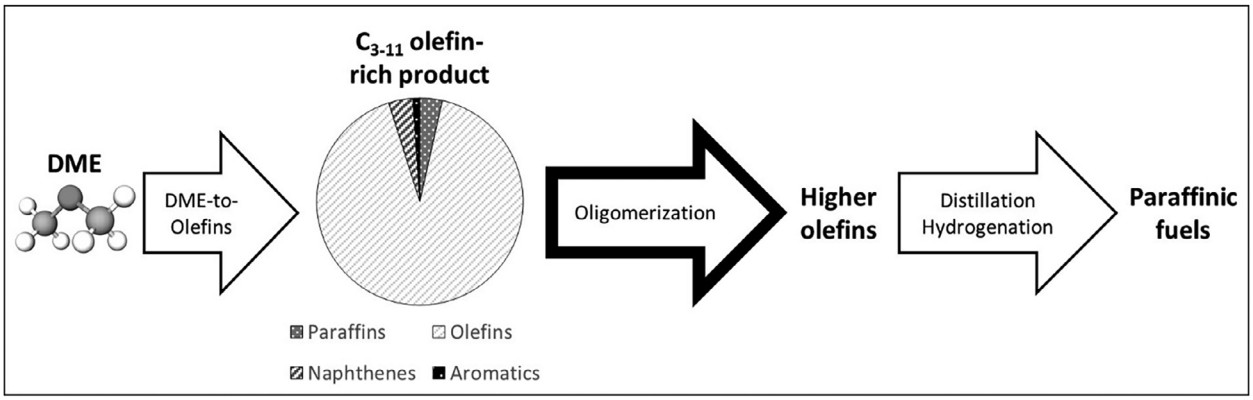

FIGURE 1 | Process chain for the production of paraffinic fuels from DME through olefin oligomerization (DME = dimethyl ether).

hydrocarbons [7, 8, 25]. Nevertheless, the increasing demand for fuel within the heavy-duty transport sector has shifted the focus of this process towards the production of sustainable aviation fuels (SAF) and diesel fuel [26, 27]. Recently, Fuchs et al. demonstrated the successful production of SAF by co-oligomerization of light olefins, using an MtO surrogate consisting of ethylene, propylene, and 1-butylene as the reactant stream. A jet fuel selectivity of 85% on nickel/Siralox-40 catalysts was achieved [28]. In that study, however, the feed composition was restricted to light olefins C_2–C_4, thereby not fully exploiting the potential impact of higher olefins on jet and diesel fuel production.

Moreover, homo-oligomerization of individual higher olefins (C_{6+}) has been reported for various catalyst systems [29–32]. Sanati et al. investigated the oligomerization of 1-hexene and 1-octene over solid acid catalysts such as H-ZSM-5 and amorphous silica–alumina at 200–300°C in fixed-bed reactors, demonstrating high conversions and the formation of C_{12+} oligomers in the boiling range of diesel fuel [29]. Sanderson et al. reported a liquid-phase oligomerization process for individual C_6–C_{12} olefins under mild conditions, yielding branched oligomers suitable as fuels and lubricants [30]. De Klerk examined the oligomerization of 1-decene and 1-dodecene over homogeneous Lewis and Brønsted acid catalysts at 20–150°C and showed that these feeds can be converted to high-viscosity oligomers and paraffins in the range of middle distillate [31]. These studies highlight that higher 1-olefins can be efficiently converted to high-quality paraffinic hydrocarbons suitable for jet or diesel fuel applications, with favorable cold flow properties and energy densities [29–32]. However, most of the work deals with either single higher olefins or relatively simple olefin mixtures and does not reflect the compositional complexity of the DtO product mentioned above [15], which contains a mixture of lower and higher olefins, paraffins, and a small amount of aromatics.

Integrating higher olefins in the oligomerization process is a promising strategy for increasing the overall SAF and diesel fuel selectivity [33]. Recently, Dubray et al. emphasized the importance of feedstocks on the quality of SAF through experimentally derived kinetic modeling [34, 35]. It is reported that to maximize the SAF range hydrocarbons along with premium quality, the co-feeding of higher olefins and light olefins like C_3–C_4 is a very promising solution. Additionally, Kuechler et al. achieved a selectivity above 40% towards hydrocarbons with a chain length of ten or more carbon atoms (C_{10+}) by oligomerizing olefins in the range of C_4–C_6, along with a recycle stream of C_4–C_{10} olefins, over ZSM-5 zeolites [36]. Although this work demonstrates the feasibility of the co-oligomerization of C_4–C_{10} olefins, the influence of specific higher olefins in the feedstock, such as hexenes and octenes, on product distribution and fuel properties is not discussed.

In addition to olefin chain length and distribution, real MtO/DtO product streams contain various non-olefinic components. Depending on the catalyst and operating conditions, paraffins and aromatics can be formed as secondary products via hydrogen transfer and aromatization pathways [2, 3, 11, 13]. These constituents are expected to affect oligomerization behavior, for instance by diluting the olefinic reactants or competing for adsorption sites [21, 22]. Despite their practical relevance, the influence of such typical impurities on the oligomerization of DtO-derived olefin mixtures has scarcely been addressed in the past. Most experimental studies employ olefin feeds without non-olefinic components, and the potential impact of paraffinic and aromatic co-feeds on activity, selectivity, and fuel quality is still not fully understood.

Figure 1 presents the complete process chain considered in this work, starting from DME, which is converted in a new DtO process to C_3–C_{11} olefins [15] and continuing with olefin oligomerization. The resulting mixture containing higher olefins is subsequently separated into the desired boiling range fractions and may undergo hydrogenation, yielding paraffinic fuels with minimal aromatic contents. To the best of our knowledge, there is no experimental work on the oligomerization of C_3–C_{11} olefin mixtures that explicitly incorporate higher olefins from an upstream DtO process. The aim of this work is to bridge this gap by experimentally investigating the oligomerization of increasingly complex olefin feeds that resemble DtO product mixtures. The main research topics of this study are

i. Investigating the influence of olefin feed composition on the oligomerization process by gradually increasing feed complexity from mixtures of lower olefins to mixtures of lower and higher olefins.

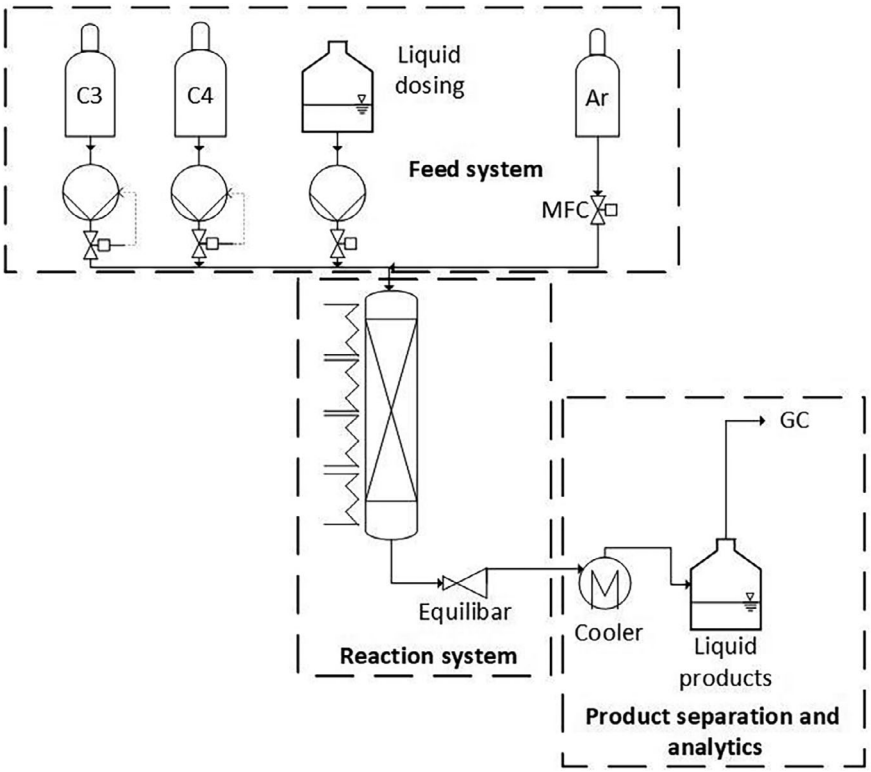

FIGURE 2 | Simplified flow diagram of the laboratory plant for continuous oligomerization. GC, gas chromatography; MFC, mass flow controller.

ii. Assessing the effect of typical impurities originating from DtO processes, by co-feeding the representative model compounds hexane for paraffins and *p*-xylene for aromatics.

iii. Evaluating the resulting hydrogenated product fractions with respect to the relevant jet and diesel fuel standards.

2 | Materials and Methods

2.1 | Reactor and Experimental Setup

The oligomerization experiments were conducted in a continuously operating laboratory fixed-bed reactor system (Figure 2). A conventional mass flow controller (MFC) was used to dose argon (99.999%, Air Liquide) into the reactor. Moreover, three conventional HPLC pumps (Knauer, Flusys) in combination with Coriolis mass flow meters (Bronkhorst) were used to dose propylene and 1-butylene as liquefied gases and a mixture of liquid olefins at ambient pressure. The corresponding propylene and 1-butylene piping was cooled to prevent evaporation. The reactants were fed in a tubular reactor with a 16 mm inner diameter made of 316Ti stainless steel. Additionally, four independent controllable heating zones were used to heat the reactor. The reaction pressure was maintained using a membrane-based backpressure regulator (Equilibar). The synthesized reaction products were cooled down in a condenser to −5°C, and the liquid products (C_{5+}) were collected in a vessel. Uncondensed gases (propylene and butylenes) were analyzed by an online gas chromatograph (GC, Hewlett-Packard 5890) equipped with an Rt-Alumina BOND/Na_2SO_4 column (30 m, 0.53 mm ID, 10 µm from Restek) and a thermal conductivity detector. The oven program of the GC-TCD system started at 120°C, and then the temperature was increased with a ramp of 30°C min^{-1} to 160°C.

The commercially available mesoporous catalyst SIRALOX 40 HPV (Sasol), with a Si/Al ratio of 0.67, was used for all experiments. The acid and surface properties of this material were extensively studied by Betz et al. [19] and Fuchs et al. [28]. Prior to the experiment, the catalyst was calcined at 550°C for 5 h. Afterwards, the catalyst powder was compressed and sieved to obtain a particle size between 250 and 500 µm. Every experiment was carried out with 15 g of fresh catalyst. Before filling the catalyst into the reactor, it was mixed with ten times its volume of silicon carbide, to enable isothermal operation. Before starting the experiments, the catalyst was heated at 300°C for 8 h under a 200 mL_N min^{-1} argon flow.

A mixture of the light olefins propylene (99.5%, Air Liquide) and 1-butylene (99.4%, Air Liquide) was used as a reference mixture before its complexity was expanded by adding higher olefins such as 1-hexene (97%, Thermo Scientific) and 1-octene (97%, Thermo Scientific). Moreover, paraffins and aromatics were mixed to the feed to assess the influence of impurities from previous olefin syntheses on the oligomerization process. Hexane (95%, Fisher Chemicals) and *p*-xylene (99%, Alfa Aesar) were selected as the paraffinic and aromatic model components, respectively. According to the DtO process of Niethammer et al. [15], the feed contains 1 wt.% aromatics. These low concentrations in aromatics cannot be detected by the applied analytics. As a consequence, no *p*-xylene concentration can be measured in the liquid product, and the influence of *p*-xylene on the oligomerization process can only be detected by the change in the product distribution.

TABLE 1 | Detailed feed compositions for the oligomerization experiments.

	Olefin composition				Total feed composition		
Experiment	Propylene [mol%]	1-Butylene [mol%]	1-Hexene [mol%]	1-Octene [mol%]	Olefins [wt.%]	Hexane [wt.%]	*p*-Xylene [wt.%]
exp#1	50	50	0	0	100	0	0
exp#2	25	25	30	20	100	0	0
exp#3	25	25	30	20	90	10	0
exp#4	25	25	30	20	90	9	1
exp#5	25	25	30	20	90	9	1

The complexity of the used feedstock gradually increases from lower olefins in Experiment 1 (exp#1) to a mixture of higher and lower olefins, including aromatics and paraffinic impurities, in Experiment 5 (exp#5). The feed compositions for all experiments are listed in Table 1.

The experiments were performed applying a weight hourly space velocity (*WHSV*) of 2 h^{-1} and a pressure of 20 bar. Experiments 1–4 (exp#1–4) were conducted with a reaction temperature of 120°C and Experiment 5 (exp#5) with a temperature of 160°C. All experiments were performed for 32 h, and a liquid sample was taken from the liquid collected within the first 8 h. Liquid analysis was performed on an offline GC (Agilent 6890) using a DB-1 column (60 m, 0.25 mm, 0.5 µm from Agilent) and a flame ionization detector (FID). The oven program of the GC-FID system started at 31°C with a hold time of 5 min. Afterwards, the temperature was increased with a ramp of 2°C min^{-1} to 125°C, and then the temperature ramp was increased to 15°C min^{-1} up to a temperature of 280°C, which was held for 15 min. The chain length distributions were analyzed by separating fractions with up to 12 carbon atoms and lumping the remaining hydrocarbons in one C_{13+} fraction. With regard to the feed, 20 vol.% of argon was added as balancing gas. After every experiment, the reactor was depressurized, and the reaction system was flushed with 200 mL_N min^{-1} argon to remove the remaining hydrocarbons from the system.

2.2 | Upgrading of Oligomerization Products

The obtained oligomerization products were upgraded by distillation and hydrogenation. In a first distillation at ambient pressure, the middle distillate fraction was separated from the oligomerization product. The condensate, which is generated with a top vapor temperature below 130°C, is referred as the gasoline fraction. The bottom product is the middle distillate, which was hydrogenated in a semi-batch reactor at 30 bar and 80°C using a 5% Pd/C catalyst. The catalyst mass used in the batch autoclave was 0.75 wt.% of the middle distillate. The hydrogen consumption to maintain the reaction pressure of 30 bar was recorded. The kerosene fraction was separated from the hydrogenated middle distillate at 10 mbar. The condensate, which was produced with a top vapor temperature below 160°C, is referred as the kerosene fraction. The mass of each fuel fraction was recorded.

The quality of both kerosene fraction and diesel fuel fraction was evaluated by measuring the density (Mettler Toledo) as well as the distillation behavior (OptiPMD, PAC). The cold flow properties of the kerosene fractions were measured by ASG Analytik-Service AG and characterized by the viscosity at −20°C (ASTM D7042) and −40°C (ASTM D7042) and the freezing point (ASTM D5972). As there is no annex in the ASTM D7566-24d for the Methanol-to-Jet fuel process route, ASTM D7566-22a Annex 5 (Alcohol-to-Jet fuel, AtJ) was used for comparison of the kerosene fractions as it includes similar process steps [25].

For the diesel fuel fraction, the cetane numbers were measured by ASG Analytik-Service AG (DIN EN 17155). The viscosity of the diesel fuel fraction was determined at 40°C (modular compact rheometer, Anton Paar). The measured fuel parameters were compared to the DIN EN 590 standard for fossil diesel fuel, DIN EN 15940 class B for paraffinic diesel fuel, and ISO 8217 DMB grade, which is often used for benchmarking alternative marine diesel fuels [37–39].

3 | Results and Discussion

3.1 | Influence of Feed Composition and Impurities on the Oligomerization Reaction

The influence of the feedstock, the reaction temperature, and paraffinic and aromatic impurities on the chain length distribution is shown in Figure 3. Using a mildly acidic catalyst and relatively low reaction temperatures of 120°C and 160°C, the formation of aromatics is unlikely. Consequently, only olefins with different chain lengths are synthesized.

For all experiments, a broad range of reaction products can be observed. A similar trend has been reported by Fuchs et al. for the co-oligomerization of ethylene, propylene, and 1-butylene. This observation can be linked to a broad variety of oligomerization routes, which can occur from a feed including several olefins with different chain lengths [28].

The feedstock comprising lower olefins (exp#1) favors the formation of oligomerization products with a comparatively short chain length. This feedstock provides the lowest C_{13+} fraction of all experiments but the highest selectivity (S_i) for molecules with chain lengths between 5 and 12 carbon atoms ($S_{5–12}$) (Table 2). This trend is especially pronounced in the selectivity for hydrocarbons with a chain length between 9 and 12 carbon atoms ($S_{9–12}$), which belong to the jet fuel range. This means that higher olefins in the feedstock, as in exp#2, are increasing the share of higher hydrocarbons (S_{13+}).

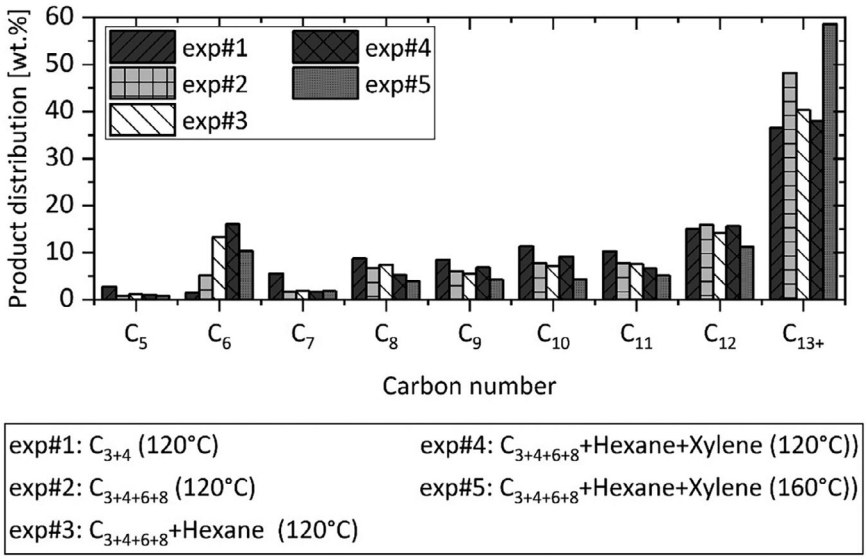

FIGURE 3 | The influence of different feedstocks, temperature, paraffinic, and aromatic impurities on the product distribution after 8 h. Reaction conditions: $p_{total} = 20$ bar, $WHSV = 2\ h^{-1}$.

TABLE 2 | Selectivity to different chain lengths.

Experiment	S_{5-12} [wt.%]	S_{9-12} [wt.%]	S_{9+} [wt.%]	S_{13+} [wt.%]
exp#1	63.4	45.0	81.5	36.5
exp#2	51.8	37.4	85.6	48.2
exp#3	57.8	34.2	74.5	41.9
exp#4	62.0	38.2	76.1	38.0
exp#5	41.3	24.7	83.2	58.5

The effect of higher olefins on the competitive dimerization of olefins can be discussed between two poles. If the dimerization rate of olefins for the single component homo-oligomerization is regarded, the dimerization rate decreases with increasing chain length [40, 41]. On the basis of this observation, it is expected that the incorporation of higher olefins should shift the product distribution towards products with shorter chain lengths due to decreased reactivity. On the other hand, the chain length of the dimerization products is increasing with increasing chain length of the olefin feedstock. Consequently, the incorporation of higher olefins enables oligomerization routes, which favor longer oligomers. Compared to lower olefins, higher olefins need fewer oligomerization steps to form hydrocarbons with the same chain length; for example, a C_{12} hydrocarbon can be considered a propylene tetramer, a butylene trimer, or a hexene dimer. For the experiments performed in this study, the effect of decreased reactivity, due to the incorporation of higher olefins, is outweighed by the formation of longer reaction products.

The higher olefins increase the diesel fuel fraction of the oligomerization product. The formation of hydrocarbons in the diesel fuel range has been reported for 1-hexene and 1-octene oligomerization by Klerk et al. using different zeolite and alumina-silicate catalysts and applying temperatures between 100°C and 230°C [31]. However, the usage of higher olefins in the oligomerization process can also lead to hydrocarbons in the jet fuel range. If the selectivity towards hydrocarbons in the jet fuel and diesel fuel range (S_{9+}) is regarded, a small increase of 4.1 wt.% is observed for exp#2.

Analyzing the influence of the impurities in the feedstock reveals that the presence of hexane as a paraffinic impurity, as well as the combined addition of hexane and *p*-xylene as paraffinic and aromatic impurity, respectively, leads to a reduction in the C_{13+} fraction (Table 2, exp#2–4). It is assumed that both types of impurities act as inert components reducing the olefin concentration on the catalyst. Therefore, the reaction rate is decreased, and fewer oligomerization reactions occur, resulting in a smaller C_{13+} fraction. This trend is also represented in the selectivity towards hydrocarbons in the C_{9+} range.

The reaction temperature has a significant influence on the product spectrum (exp#5). Exothermic oligomerization is a well-known reaction being in equilibrium with endothermic cracking reactions [42]. Le Chatelier's principle predicts that an increase in temperature may promote cracking reactions, leading to a shift in the chain length distribution towards shorter hydrocarbons. The temperature variation in this work is showing an opposing trend. If the reaction temperature is raised from 120°C (exp#4) to 160°C (exp#5), selectivity towards the C_{13+} fraction rises by 10 wt.%. Accordingly, the oligomerization reaction below 160°C is not controlled by thermodynamic equilibrium. Instead, it is governed by kinetic limitations, which are decreasing with temperature according to the Arrhenius law. A similar trend was observed by Coelho et al. studying 1-butylene oligomerization over ZSM-5 zeolite, observing that cracking reactions rapidly increase for temperatures above 200°C [21].

3.2 | Evaluation of Fuel Quantity

On the basis of the chain length distributions and selectivities from Figure 3 and Table 2, a detailed analysis of the fuel quantity

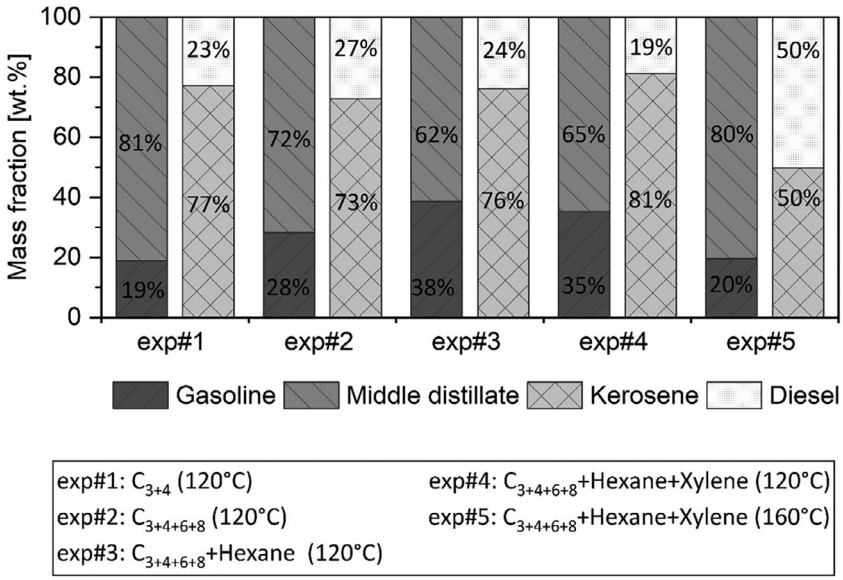

FIGURE 4 | Fractionation of the liquid products (C_{5+}) in gasoline ($T_{Vapor} \leq 130°C$), kerosene ($T_{Vapor} \leq 160°C$ at 10 mbar), and diesel fuel ($T_{Vapor} > 160°C$ at 10 mbar).

is not possible. Hydrocarbons in the C_{9+} and C_{13+} fractions can belong to the kerosene or diesel fuel fractions. Consequently, the oligomerization products were analyzed in terms of fuel quantity by separating them through distillation into a gasoline ($T_{Vapor} \leq 130°C$), kerosene ($T_{Vapor} \leq 160°C$ at 10 mbar), and diesel fuel fraction ($T_{Vapor} > 160°C$ at 10 mbar) and calculating their mass fractions (Figure 4). After this separation, further investigations on the fuel properties of the kerosene and diesel fuel fractions were carried out. The quality of the gasoline fraction was not analyzed, as it could rather be used as a recycle stream, increasing the middle distillate fraction of the overall process. According to their boiling points, unreacted 1-hexene and 1-octene in exp#2–5 are separated into the liquid product, which increases the gasoline fraction while reducing the middle distillate fraction. To quantify the share of kerosene and diesel fuel, the middle distillate composition is regarded independently, eliminating the influence of unreacted 1-hexene and 1-octene. Due to their inertness, the impurities in the feedstock are also separated into the fuel fractions according to their boiling points. Hexane is increasing the gasoline fraction while *p*-xylene is increasing the kerosene fraction.

The trends of the S_{13+} fraction can be seen from the obtained diesel fuel yield within the middle distillate. If exp#1 and exp#2 are compared in particular, an increase in the diesel fuel yield can be observed. As already shown in Section 3.1, higher olefins in the feedstock are promoting longer chain hydrocarbons in the diesel fuel range. However, the inert components in exp#3 and exp#4 are decreasing the yield of diesel fuel, as they reduce the amount of longer chain hydrocarbons (see Section 3.1). In contrast to C_{13+} selectivity, a clear trend of C_9–C_{12} selectivity cannot be seen from the kerosene yield. Higher kerosene yields do not necessarily correspond to a higher selectivity towards C_9–C_{12} (Table 2).

The diesel fuel fraction significantly increases with the temperature (exp#5), whereas the shares of the kerosene and the gasoline fractions decrease. This effect can be attributed to the enhancement of reaction kinetics, promoting the formation of higher hydrocarbons as discussed in Section 3.1. Finally, it can be concluded that the reaction temperature is the main factor governing diesel fuel and middle distillate yield, overweighing the influences of the oligomerization feedstock and impurities in the feed.

3.3 | Evaluation of Kerosene Quality

As shown in Section 3.2, the kerosene fraction is the largest fraction in all experiments. The quality of the kerosene fraction was assessed by comparison with the ASTM D7566 22a Annex 5 standard for AtJ (Table 3). Density, flash point, freezing point, viscosity, and the distillation behavior were analyzed as these parameters strongly correlate with the chain length distributions of the oligomerization products [43]. Although all the kerosene fractions, except the fraction from exp#1, comply with the analyzed standard parameters, differences in the fuel quality can be observed. The experiments with impurities in the feedstock (exp#3 and exp#4) yield kerosene fractions with a lower viscosity than the kerosene fractions obtained from exp#1, exp#2, and exp#5. The density decreases from exp#1 to exp#2 before it increases from exp#2 to exp#5. However, no distinct correlation between chain length distribution and fuel quality could be observed.

3.4 | Evaluation of Diesel Fuel Quality

This work shows that temperature is the main factor governing the diesel fuel quantity (Section 3.2). On the basis of this, the quality of the diesel fuel from exp#5, which exhibits the highest diesel fuel yield, is assessed and compared with the quality of the diesel fuel from exp#4. The measured values for the diesel fuel fraction are shown in Table 4. Density, cetane number, viscosity, and the distillation behavior were analyzed as they significantly correlate with the chain length distributions [43]. The distillation behavior of both samples shows that the distilled volumes at 250°C and 350°C meet the standards for fossil and

TABLE 3 | Comparison of selected kerosene properties to the ASTM D7566 22a Annex 5 standard.

Experiment/Standard	Density at 15°C [kg m^{-3}]	Flash point [°C]	Freezing point [°C]	Viscosity at −20°C [mm^2 s^{-1}]	Viscosity at −40°C [mm^2 s^{-1}]	T_{10}[a] [°C]	T_{100}[b] [°C]	T_{90}–T_{10}[c] [°C]
exp#1	776.1	43	<−60	4.7	9.7	171.0	260.0	54.4
exp#2	760.9	43	<−90	6.8	8.8	162.8	241.0	62.6
exp#3	763.5	46	<−90	3.7	7.3	166.2	249.4	63.3
exp#4	766.0	44	<−90	3.7	7.2	165.7	255.4	67.7
exp#5	769.5	51	<−90	4.7	10.1	175.6	250.3	58.1
ASTM D7566 22a								
Min.	730	38	—	—	—	—	—	21
Max.	770	—	−40	8	12	205	300	—

[a]Temperature at which 10 vol.% is distilled.
[b]Final boiling point.
[c]Temperature difference between T_{90} and T_{10}.

TABLE 4 | Comparison of selected diesel fuel properties to the diesel fuel standards DIN EN 590, DIN EN 15940, and ISO 8217.

Experiment/Standard	Density at 15°C [kg m^{-3}]	Cetane number [–]	Viscosity at 40°C [mm^2 s^{-1}]	Volume fraction distilled at 250°C [vol.%]	Volume fraction distilled at 350°C [vol.%]	T_{95}[a] [°C]
exp#4	828.6	38.2	7.8	0	93.5	356.7
exp#5	826.1	42.1	8.6	0	86.2	373.4
DIN EN 590						
Min.	820.0	51	2.0	—	85	—
Max.	845.0	—	4.5	<65	—	360.0
DIN EN 15940 class B						
Min.	780.0	51	2.0	—	85	—
Max.	810.0	—	4.5	<65	—	360.0
ISO 8217 DMB grade						
Min.	—	—	2.0	—	—	—
Max.	900.0	—	11.0	—	—	—

[a]Temperature at which 95 vol.% is distilled.

paraffinic diesel fuel. The temperature at which 95 vol.% of the diesel fuel fraction is distilled is too high in the case of exp#5 and results from a high amount of high boiling components. The increase in higher hydrocarbons due to the temperature rise from 120°C to 160°C is also reflected in the distillation behavior as shown in Section 3.1. The initial boiling point is above 250°C for both samples, indicating that no low boiling components are included. This aspect is strongly linked with other fuel parameters like density and viscosity. Although the density is complying with the standard for fossil diesel fuel and marine diesel fuel DMB grade, it is too high for paraffinic diesel fuel. Low-boiling components usually exhibit shorter carbon chain lengths, resulting in lower densities and viscosities. Regarding the cetane numbers of both samples, the values are too low. The cetane number is strongly influenced by the chain length and the branching of the molecules, as longer chain lengths and less branching cause high cetane numbers [44]. Consequently, high cetane numbers are expected as the samples contain no low-boiling hydrocarbons with short chain lengths. However, as the measurements show an opposing trend, it is assumed that highly branched hydrocarbons in the diesel fuel fraction are significantly decreasing the cetane number, thus outweighing the effect of chain length.

In general, olefin oligomerization provides a broad variety of reaction products within the jet and diesel fuel range. As the chain length ranges for jet and diesel fuels overlap, co-production of both fuels remains a challenge. In this work, the distillation cut was set to obtain high kerosene quality. Different distillation cuts can be investigated in order to improve diesel fuel quality while maintaining kerosene quality in accordance with the ASTM D7566 22a Annex 5 standard.

4 | Conclusion

The present study shows that the incorporation of higher olefins into the heterogeneously catalyzed oligomerization of light olefins is feasible, increasing the formation of higher hydrocarbons (C_{13+}). The kerosene fraction was the largest product fraction in all experiments conducted at 120°C, and many fuel properties such as density, flash point, freezing point, viscosity, and distillation behavior complied with the ASTM D7566 22a standard, highlighting its potential use as SAF. The diesel fuel properties did mostly not comply with the DIN EN 590 and DIN EN 15940 class B standards, whereas some parameters met the requirements of the ISO 8217 DMB grade for marine diesel fuel.

Moreover, the influence of paraffinic and aromatic impurities on oligomerization catalyzed by a SIRALOX 40 catalyst was investigated. Paraffinic and aromatic impurities are inert, reducing the olefin concentration on the catalyst and thus reducing the reaction rate. Therefore, fewer oligomerization steps occur on the catalyst, decreasing the formation of higher hydrocarbons.

The temperature has been identified as the main parameter to influence the product distribution and the fuel share, overweighing the influence of the feed composition as well as paraffinic and aromatic impurities in the feedstock. The increase in reaction temperature from 120°C to 160°C enhanced the C_{13+} fraction by 10.3 wt.%, thereby increasing the diesel fuel yield from 19 to 50 wt.%.

It can be concluded that the oligomerization of a DtO product surrogate comprising lower and higher olefins has been successfully demonstrated. This shows a promising potential to couple DME-based olefin synthesis with olefin oligomerization for the production of hydrocarbon fuels. This pathway seems to be suitable in particular for the production of SAF, which is addressed in ongoing work.

Nomenclature

Symbols

C_i	olefin with i carbon atoms, –
p	pressure, bar
S_i	selectivity to i carbon atoms, %
T	temperature, °C
T_V	temperature at which V vol.% is distilled, °C
T_{Vapor}	vapor temperature, °C
$WHSV$	weight hourly space velocity, h^{-1}

Acknowledgments

Financial support from the Ministry of Transport Baden-Württemberg for the joint research project "E-Fuels for the LÄND" is gratefully acknowledged.

Open access funding enabled and organized by Projekt DEAL.

References

1. Bundesministerium Für Forschung, Technologie Und Raumfahrt, *Hightech Agenda Deutschland* (Bundesministerium Für Forschung, Technologie Und Raumfahrt, 2025).

2. T. Cordero-Lanzac, A. G. Gayubo, A. T. Aguayo, and J. Bilbao, "The MTO and DTO Processes as Greener Alternatives to Produce Olefins: A Review of Kinetic Models and Reactor Design," *Chemical Engineering Journal* 494 (2024): 152906, https://doi.org/10.1016/j.cej.2024.152906.

3. S. Xu, Y. Zhi, J. Han, et al., "Advances in Catalysis for Methanol-to-Olefins Conversion," *Advances in Catalysis* 61 (2017): 37–122, https://doi.org/10.1016/bs.acat.2017.10.002.

4. N. Dahmen, U. Arnold, N. Djordjevic, et al., "High Pressure in Synthetic Fuels Production," *Journal of Supercritical Fluids* 96 (2015): 124–132, https://doi.org/10.1016/j.supflu.2014.09.031.

5. Z. Wang, T. He, J. Li, et al., "Design and Operation of a Pilot Plant for Biomass to Liquid Fuels by Integrating Gasification, DME Synthesis and DME to Gasoline," *Fuel* 186 (2016): 587–596, https://doi.org/10.1016/j.fuel.2016.08.108.

6. Z. Azizi, M. Rezaeimanesh, T. Tohidian, and M. R. Rahimpour, "Dimethyl Ether: A Review of Technologies and Production Challenges," *Chemical Engineering and Processing - Process Intensification* 82 (2014): 150–172, https://doi.org/10.1016/j.cep.2014.06.007.

7. S. Polierer, D. Guse, S. Wild, et al., "Enhanced Direct Dimethyl Ether Synthesis From CO_2-Rich Syngas With Cu/ZnO/ZrO_2 Catalysts Prepared by Continuous Co-Precipitation," *Catalysts* 10, no. 8 (2020): 816, https://doi.org/10.3390/catal10080816.

8. N. D. Otalvaro, G. Sogne, K. H. Delgado, S. Wild, S. Pitter, and J. Sauer, "Kinetics of the Direct DME Synthesis From CO_2 Rich Syngas Under Variation of the CZA-to-γ-Al_2O_3 Ratio of a Mixed Catalyst Bed," *RSC Advances* 11, no. 40 (2021): 24556–24569, https://doi.org/10.1039/D1RA03452A.

9. P. Pérez-Uriarte, A. Ateka, A. T. Aguayo, A. G. Gayubo, and J. Bilbao, "Kinetic Model for the Reaction of DME to Olefins Over a HZSM-5 Zeolite Catalyst," *Chemical Engineering Journal* 302 (2016): 801–810, https://doi.org/10.1016/j.cej.2016.05.096.

10. P. N. Plessow, A. Smith, S. Tischer, and F. Studt, "Identification of the Reaction Sequence of the MTO Initiation Mechanism Using Ab Initio-Based Kinetics," *Journal of the American Chemical Society* 141, no. 14 (2019): 5908–5915, https://doi.org/10.1021/jacs.9b00585.

11. S. Lin, Y. Zhi, Z. Liu, et al., "Multiscale Dynamical Cross-Talk in Zeolite-Catalyzed Methanol and Dimethyl Ether Conversions," *National Science Review* 9, no. 9 (2022): nwac151, https://doi.org/10.1093/nsr/nwac151.

12. S. Lee, M. Gogate, and C. J. Kulik, "Methanol-To-Gasoline vs. DME-To-Gasolne Ii. PROCESS Comparison and Analysis," *Fuel Science and Technology International* 13, no. 8 (1995): 1039–1057, https://doi.org/10.1080/08843759508947721.

13. M. Yang, D. Fan, Y. Wei, P. Tian, and Z. Liu, "Recent Progress in Methanol-to-Olefins (MTO) Catalysts," *Advanced Materials* 31, no. 50 (2019): 1902181, https://doi.org/10.1002/adma.201902181.

14. J. Zhong, J. Han, Y. Wei, and Z. Liu, "Catalysts and Shape Selective Catalysis in the Methanol-to-Olefin (MTO) Reaction," *Journal of Catalysis* 396 (2021): 23–31, https://doi.org/10.1016/j.jcat.2021.01.027.

15. B. Niethammer, U. Arnold, and J. Sauer, "Suppressing the Aromatic Cycle of the Dimethyl Ether to Hydrocarbons Reaction on Zeolites," *Applied Catalysis A: General* 651 (2023): 119021, https://doi.org/10.1016/j.apcata.2023.119021.

16. B. Niethammer, F. Zormpa, G. T. Hoang, et al., "Conversion of Dimethyl Ether to Hydrocarbons Catalyzed by Pd-Loaded *MRE Zeolites," *Catalysis Today* 453 (2025): 115258, https://doi.org/10.1016/j.cattod.2025.115258.

17. B. Niethammer, U. Arnold, and J. Sauer, Process for Converting Dimethyl Ether or Methanol to Hydrocarbons Low in Aromatic Compounds, Using a Palladium-Loaded Zeolite Catalyst, (WIPO, PCT) WO2023117271A1 (2023).

18. A. V. Lavrenov, T. R. Karpova, E. A. Buluchevskii, and E. N. Bogdanets, "Heterogeneous Oligomerization of Light Alkenes: 80 Years in Oil Refining," *Catalysis in Industry* 8, no. 4 (2016): 316–327, https://doi.org/10.1134/S2070050416040061.

19. M. Betz, C. Fuchs, T. A. Zevaco, U. Arnold, and J. Sauer, "Production of Hydrocarbon Fuels by Heterogeneously Catalyzed Oligomerization of Ethylene: Tuning of the Product Distribution," *Biomass and Bioenergy* 166 (2022): 106595, https://doi.org/10.1016/j.biombioe.2022.106595.

20. S. Moussa, M. A. Arribas, P. Concepción, and A. Martínez, "Heterogeneous Oligomerization of Ethylene to Liquids on Bifunctional Ni-Based Catalysts: The Influence of Support Properties on Nickel Speciation and Catalytic Performance," *Catalysis Today* 277 (2016): 78–88, https://doi.org/10.1016/j.cattod.2015.11.032.

21. A. Coelho, G. Caeiro, M. A. N. D. A. Lemos, F. Lemos, and F. R. Ribeiro, "1-Butene Oligomerization Over ZSM-5 Zeolite: Part 1 – Effect of Reaction Conditions," *Fuel* 111 (2013): 449–460, https://doi.org/10.1016/j.fuel.2013.03.066.

22. C. P. Nicholas, "Applications of Light Olefin Oligomerization to the Production of Fuels and Chemicals," *Applied Catalysis A: General* 543 (2017): 82–97, https://doi.org/10.1016/j.apcata.2017.06.011.

23. W. Monama, E. Mohiuddin, B. Thangaraj, M. M. Mdleleni, and D. Key, "Oligomerization of Lower Olefins to Fuel Range Hydrocarbons Over Texturally Enhanced ZSM-5 Catalyst," *Catalysis Today* 342 (2020): 167–177, https://doi.org/10.1016/j.cattod.2019.02.061.

24. K. Toch, J. W. Thybaut, M. A. Arribas, A. Martínez, and G. B. Marin, "Steering Linear 1-Alkene, Propene or Gasoline Yields in Ethene Oligomerization via the Interplay Between Nickel and Acid Sites," *Chemical Engineering Science* 173 (2017): 49–59, https://doi.org/10.1016/j.ces.2017.07.025.

25. M. Rumizen, *Biokerosene*, ed. M. Kaltschmitt and U. Neuling (Springer Berlin Heidelberg, 2018).

26. N. Gray, S. McDonagh, R. O'Shea, B. Smyth, and J. D. Murphy, "Decarbonising Ships, Planes and Trucks: An Analysis of Suitable Low-Carbon Fuels for the Maritime, Aviation and Haulage Sectors," *Advances in Applied Energy* 1 (2021): 100008, https://doi.org/10.1016/j.adapen.2021.100008.

27. S. Wandelt, Y. Zhang, and X. Sun, "Sustainable Aviation Fuels: A Meta-Review of Surveys and Key Challenges," *Journal of the Air Transport Research Society* 4 (2025): 100056, https://doi.org/10.1016/j.jatrs.2024.100056.

28. C. Fuchs, U. Arnold, and J. Sauer, "Synthesis of Sustainable Aviation Fuels via (Co–)Oligomerization of Light Olefins," *Fuel* 382 (2025): 133680, https://doi.org/10.1016/j.fuel.2024.133680.

29. M. Sanati, C. Hörnell, and S. G. Järäs, *Catalysis*, 1st ed., ed. J. J. Spivey (Royal Society of Chemistry, 1999).

30. J. R. Sanderson and J. F. Knifton, Process for Oligomerizing Olefins Using Halogenated Phosphorous-Containing Acid on Montmorillonite Clay, US5191130A (1993).

31. A. De Klerk, "Oligomerization of 1-Hexene and 1-Octene Over Solid Acid Catalysts," *Industrial & Engineering Chemistry Research* 44, no. 11 (2005): 3887–3893, https://doi.org/10.1021/ie0487843.

32. B. G. Harvey and H. A. Meylemans, "1-Hexene: A Renewable C6 Platform for Full-Performance Jet and Diesel Fuels," *Green Chemistry* 16, no. 2 (2014): 770–776, https://doi.org/10.1039/C3GC41554F.

33. A. Elwalily, E. Verkama, F. Mantei, et al., "Sustainable Aviation Fuel Production via the Methanol Pathway: A Technical Review," *Sustain Energy Fuels* 9, no. 19 (2025): 5151–5180, https://doi.org/10.1039/D5SE00231A.

34. F. J. Dubray, V. Paunovic, and J. A. Van Bokhoven, "Optimization of Sustainable Aviation Fuel Production Through Experiment-Driven Modeling of Acid-Catalyzed Oligomerization," *ACS Sustainable Chemistry & Engineering* 12, no. 48 (2024): 17590–17599, https://doi.org/10.1021/acssuschemeng.4c08240.

35. F. Dubray, V. Paunović, M. Ranocchiari, and J. A. Van Bokhoven, "Production of Jet-Fuel-Range Olefins via Catalytic Conversion of Pentene and Hexene Over Mesoporous Al-SBA-15 Catalyst," *Journal of Industrial and Engineering Chemistry* 114 (2022): 409–417, https://doi.org/10.1016/j.jiec.2022.07.030.

36. K. H. Kuechler, S. H. Brown, A. A. Verberckmoes, M. P. Puttemans, and S. E. Silverberg, Hydrocarbon Compositions Useful for Producing Fuels and Methods of Producing the Same, US7692049B2 (2010).

37. Z. Wang, T. Paulauskiene, J. Uebe, and M. Bucas, "Characterization of Biomethanol–Biodiesel–Diesel Blends as Alternative Fuel for Marine Applications," *Journal of Marine Science and Engineering* 8, no. 9 (2020): 730, https://doi.org/10.3390/jmse8090730.

38. T. Paulauskiene, M. Bucas, and A. Laukinaite, "Alternative Fuels for Marine Applications: Biomethanol-Biodiesel-Diesel Blends," *Fuel* 248 (2019): 161–167, https://doi.org/10.1016/j.fuel.2019.03.082.

39. H.-S. Jang, J.-S. Kim, M.-H. Lee, et al., "A Field-Study of the Feasibility of the Use of Biodiesel in the Marine Industry," *Journal of International Maritime Safety Environmental Affairs and Shipping* 7, no. 4 (2023): 2267905, https://doi.org/10.1080/25725084.2023.2267905.

40. W. F. Hölderich and D. Heinz, *Catalysis*, 1st ed., ed. J. J. Spivey (Royal Society of Chemistry, 1999).

41. J. C. Gee and S. T. Williams, "Dimerization of Linear Olefins on Amberlyst 15: Effects of Chain Length and Double-Bond Position," *Journal of Catalysis* 303 (2013): 1–8, https://doi.org/10.1016/j.jcat.2013.03.017.

42. S. A. Tabak, F. J. Krambeck, and W. E. Garwood, "Conversion of Propylene and Butylene Over ZSM-5 Catalyst," *AIChE Journal* 32, no. 9 (1986): 1526–1531, https://doi.org/10.1002/aic.690320913.

43. X. Wang, T. Jia, L. Pan, et al., "Review on the Relationship Between Liquid Aerospace Fuel Composition and Their Physicochemical Properties," *Transactions of Tianjin University* 27, no. 2 (2021): 87–109, https://doi.org/10.1007/s12209-020-00273-5.

44. J. Jenčík, V. Hönig, M. Obergruber, et al., "Advanced Biofuels Based on FischerTropsch Synthesis for Applications in Diesel Engines," *Materials* 14, no. 11 (2021): 3077, https://doi.org/10.3390/ma14113077.